

Laser Light Scattering Study of the Phase Transition of Poly(*N*-isopropylacrylamide) in Water. 1. Single Chain

Chi Wu* and Shuiqin Zhou

Department of Chemistry, The Chinese University of Hong Kong, Shatin, N.T., Hong Kong

Received April 4, 1995; Revised Manuscript Received September 5, 1995*

ABSTRACT: The coil-to-globule transition of a single chain of narrowly distributed ($M_w/M_n < 1.05$) high molecular weight ($M_w > 10^7$ g/mol) poly(*N*-isopropylacrylamide) in extremely dilute solutions (~ 5 $\mu\text{g/mL}$) was studied by both static and dynamic laser light scattering. The thermodynamically stable collapsed globule ($R_g/R_h = 0.97$) was observed for the first time. However, when $R_g/R_h < 0.97$, the single-chain globules were “metastable”; i.e., the globules in the solution were stable only for a finite time. Two-stage chain collapsing kinetics in the thermodynamically stable region was observed. The time scales ($\sim 10^2$ s) observed in both the chain collapsing and dissolving processes are too short to support the previously suggested high chain-knotting density inside the globule. The R_g/R_h can be as low as ~ 0.62 , lower than 0.774 predicted for a uniform density sphere. This paradox suggests that the chain density is higher at the center of the globule than that near the surface. The highly collapsed globule still contains $\sim 80\%$ water in its hydrodynamic volume.

Introduction

Three decades ago, Stockmayer first suggested that a flexible polymer chain can change from an expanded coil to a collapsed globule.¹ Since then, this prediction has been extensively studied both theoretically and experimentally.^{2–11} Most studies were concentrated on polystyrene solutions, satisfying the requirement of a very high molecular weight and narrow molecular weight distribution. Useful experimental results were obtained using static and dynamic laser light scattering (LLS)^{8–11} and interpreted by the existing theory.^{4–6}

Grosberg and Kuznetsov¹² recently concluded that the true equilibrium single-chain collapse has not yet been observed experimentally for simple uncharged homopolymers without mesogenic groups. They predicted a two-stage kinetics for the collapse of a single chain, a fast crumpling of the unknotted chain followed by a slow knotting of the collapsed polymer chain. This two-stage kinetics has recently been observed by Chu *et al.*^{13,14} in studying the single polystyrene chain collapse before its precipitation. In their experiment, dynamics LLS was employed to monitor the change of the hydrodynamic radius (R_h) of a single polystyrene chain in cyclohexane after an abrupt temperature change from 35 (the Θ temperature) to 29 °C. Their measured hydrodynamic radius distribution showed two quite different species which were attributed to single polystyrene chains and aggregates of the polystyrene chains. From the time dependence of R_h of the single chain after the abrupt temperature change, two relaxation times τ_{crum} and τ_{eq} , respectively, for the crumpled globule state and the compact globule state were reported.

The interest in this coil-to-globule transition is due both to its importance as a fundamental concept in polymer physics and solution dynamics and its relevance to many biological systems, such as protein folding¹⁵ and DNA packing.^{16–18} Thus, the investigation of the coil-to-globule transition of polymers in aqueous solution is most interesting. On the other hand, the study of aqueous polymer solutions often involves additional interaction, making theoretical development more difficult. Only a very limited number of studies

have been reported.^{19–21} All of them involve poly(*N*-isopropylacrylamide) (PNIPAM) in water.

Swollen PNIPAM gels have a sharp volume phase transition with the volume change being as much as 100-fold.²² The main driving forces for the PNIPAM phase transition are the hydrophobic and hydrophilic interactions which can be much stronger than the van de Waals interactions for polystyrene in an organic solvent. Thus, it should be easier for individual PNIPAM chains to reach a collapsed state in water than for polystyrene chains in an organic solvent. Kubota *et al.*²⁰ were the first to attempt to use a narrowly distributed PNIPAM sample to study the coil-to-globule transition in water. Their results confirmed the existence of a lower critical solution temperature (LCST, ~ 32.00 °C). They used three PNIPAM samples with $M_w > 4.10 \times 10^6$ g/mol and $M_w/M_n > 1.3$, for which they observed a limited chain collapse before the system reached thermodynamical instability, i.e., phase separation and aggregation. Meewes *et al.*²¹ went further with a PNIPAM sample ($M_w \sim 7 \times 10^6$ g/mol and $M_w/M_n \sim 1.3$) with a surfactant added to prevent phase separation. Unfortunately, the addition of the surfactant shifted the LCST to a higher temperature (~ 35 °C) and complicated the picture of coil-to-globule transition.

Recently, we studied PNIPAM in different forms including individual PNIPAM chains, lightly connected PNIPAM microgel particles, the interaction of PNIPAM chains and microgel particles with various surfactants, and a very thin PNIPAM gel film. Here, only single-chain properties will be reported. For the study of single-chain properties, a great effort was spent in the preparation of two narrowly distributed ($M_w/M_n < 1.05$) high molecular weight ($M_w > 10^7$ g/mol) PNIPAM samples. With these PNIPAM samples, we studied the coil-to-globule transition of single PNIPAM chains in extremely dilute solutions (~ 5 $\mu\text{g/mL}$) by using laser light scattering. It is well-known that, for a polydisperse sample, the species with a higher molecular weight will undergo the phase transition first, which leads the whole solution into a thermodynamically unstable region. It is also known that for a water-soluble polymer the coil-to-globule transition is easier because of a relative stronger hydrophobic interaction. As expected, with our narrowly distributed high molec-

* Abstract published in *Advance ACS Abstracts*, October 15, 1995.

ular weight, water-soluble PNIPAM in extremely dilute solutions, we were able to see the coil-to-globule transition in a relatively wide temperature range and especially very near the phase transition temperature, but without entering the two-phase region (thermodynamically unstable). This is exactly why, for the first time, we observed a thermodynamically stable PNIPAM globule, studied the single-chain collapsing and dissolving kinetics in the thermodynamically stable region, and showed that even in the highly collapsed PNIPAM globule the PNIPAM chain density is not uniform as previously suggested and much lower than that of bulk PNIPAM.

Theoretical Background

Single-Chain Collapse. For a given polymer solution, the solvent can change from a good to a Θ solvent and finally to a poor solvent, or vice versa, with temperature change. When the solvent quality is poor, a flexible polymer chain contracts. By using the modified Flory theory, the chain contraction (or collapse) has been formulated in terms of an expansion factor α [$\equiv R(T)/R(\Theta)$] by^{23,24}

$$\frac{7(1 - \alpha^2)}{3r} = \frac{1}{2}(\Theta/T)\phi + \frac{\ln(1 - \phi)}{\phi} + 1 \quad (1)$$

where $\phi \equiv \phi_0/\alpha^3$ with ϕ_0 the fraction of space occupied by chains whose radius of gyration R_g is equal to the ideal value R_g^0 ; r is the number of residues, which may be one monomer unit or a number of repeat units grouped together; and $R(T)$ and $R(\Theta)$ are the radius of gyration and hydrodynamic radius at temperature T and the Flory Θ temperature, respectively. In eq 1, ϕ has to be less than 1; i.e., $\alpha > \phi_0^{1/3}$. The maximum observed value of ϕ in this study was ~ 0.5 . If $r \rightarrow \infty$, $\phi_0 \rightarrow (19/27)^{1/2} r^{-1/2}$. In a good solvent, $\alpha > 1$ and $\phi \ll 1$. After expanding $\ln(1 - \phi)$, we can rewrite eq 1 in a more familiar form as²⁵

$$\alpha^6(1 - \alpha^2) + 0.102 + \dots = 0.180\alpha^3\tau(M_w/M_0)^{1/2} \quad (2)$$

where τ [$\equiv (T - \Theta)/\Theta$] is the reduced temperature; $[(T - \Theta)/T]$ is approximated by τ since T is near Θ ; we have replaced r by M_w/M_0 with M_w and M_0 being the mass of the polymer and that of the "residues", respectively. Equation 2 shows that, as α decreases, $\alpha^3 M_w^{1/2} \tau$ approaches a plateau if the higher-order terms can be dropped at small α and M_0 is T -independent. Moreover, eq 2 shows that $\alpha^3 M_w^{1/2} \tau$ scales as a function of $M^{1/2} \tau$.

Coil-to-Globule Transition Kinetics. In comparison with the theoretical development of equilibrium single-chain globule, little theory has been published on the kinetics of coil-to-globule transition. The proposed theories are either qualitative descriptions¹² or computer simulations with a limited chain length.²⁶ One decade ago, de Gennes²⁷ stated that if a polymer chain is quenched in a poor solvent the polymer chain will adopt a "sausage"-like conformation wherein each block of "sausage" will gradually shorten and thicken in a self-similar manner during the chain collapse. By using solvent viscosity data, the characteristic relaxation time was estimated to be in the order of $\sim 10^{-3}$ s, much shorter than the experimental value ($\sim 10^2$ s),¹⁴ if it was identified with the initial kinetics. This discrepancy may be attributed to the higher local viscosity when the polymer chain is collapsed and to possible topological

constraints and self-entanglements inside the globule which will certainly slow down the kinetics.

On the basis of the above concepts, Grosberg *et al.* qualitatively predicted that the collapse could be a two-stage process, i.e., a fast process similar to that described by de Gennes and a slow process assumed to be similar to self-reptation.²⁸ The fast collapse could be visualized as crumpling, followed by a slow knotting process. In the first process, the chain density in its occupied volume increases fast as the chain collapses, while in the second process the chain density increases much more slowly during the rearrangement of the collapsed chain in the globule. The relaxation times associated with these processes, i.e., τ_{crum} and τ_{eq} , can be written as^{12,14}

$$\tau_{\text{crum}} \propto M_w^2 \frac{\eta}{\Theta} (\alpha_{\text{crum}}/\alpha_{\text{eq}})^3 \quad (3)$$

and

$$\tau_{\text{eq}} \propto M_w^3 \frac{\eta}{\Theta} \gg \tau_{\text{crum}} \quad (4)$$

where η is the solvent viscosity and the ratio of the expansion factors $\alpha_{\text{crum}}/\alpha_{\text{eq}}$ is, like g , related to the size ratio¹²

$$g = R_{\text{crum}}/R_{\text{eq}} = (1 + \zeta)^{1/3} \quad (5)$$

where ζ is a constant. In practice, it is rather difficult to verify this two-stage collapse experimentally because the time for the polymer solution to reach temperature equilibrium after a temperature jump is longer than the relaxation times. This is why only one experimental result has been reported so far.¹⁴

Static Laser Light Scattering. The LLS theory^{29,30} has shown that for a dilute solution at a small scattering angle the weight-average molecular weight M_w can be related to the excess absolute time-averaged scattered light intensity (known as the Rayleigh ratio $[R_{\text{vv}}(q)]$) by

$$\frac{KC}{R_{\text{vv}}(q)} \approx \frac{1}{M_w} \left(1 + \frac{1}{3} \langle R_g^2 \rangle q^2 \right) + 2A_2 C \quad (6)$$

where $K = 4\pi^2 n^2 (\partial n / \partial C)^2 / (N_A \lambda_0^4)$, with N_A , n , and λ_0 being Avogadro's number, the solvent refractive index, and the wavelength of light in vacuo, respectively; $q = (4\pi n / \lambda_0) \sin(\theta/2)$ with θ being the scattering angle; C is the polymer concentration (g/mL); $\langle R_g^2 \rangle^{1/2}$ (written as R_g) is the z -average radius of gyration; and A_2 is the second virial coefficient. When $C \sim 10^{-6}$ g/mL, the term $2A_2 C$ can be dropped since $A_2 < 10^{-4}$ for PNIPAM in water. The plot of $KC/R_{\text{vv}}(q)$ vs q^2 leads to M_w and R_g , respectively, from the intercept and slope.

Dynamic Laser Light Scattering. Normally, a precise intensity-intensity time correlation function $G^{(2)}(t, q)$ in the self-beating mode is measured, which has the following form^{31,32}

$$G^{(2)}(t, q) = A[1 + \beta |g^{(1)}(t, q)|^2] \quad (7)$$

where A is a measured baseline, β , a parameter depending on the coherence of detection, t , the delay time, and $g^{(1)}(t, q)$, the normalized electric field time correlation function which can be related to the line-width distribution $G(\Gamma)$ by

$$g^{(1)}(t, q) = \int_0^\infty G(\Gamma) e^{-\Gamma t} d\Gamma \quad (8)$$

The line-width Γ is usually a function of both C and Θ , which can be expressed as³³

$$\frac{\Gamma}{q^2} = D(1 + k_d C)[1 + f(R_g q)^2] \quad (9)$$

where D is the translational diffusion coefficient, k_d is the diffusion second virial coefficient, and f is a dimensionless constant. When the solution is extremely dilute and $R_g q \ll 1$, the ratio of Γ/q^2 is approximately equal to D . $G(\Gamma)$ in eq 8 can be obtained from the Laplace inversion of the measured $G^{(2)}(t, q)$. Furthermore, at $C \rightarrow 0$ and $q \rightarrow 0$, $G(\Gamma)$ can be converted to the translational diffusion coefficient distribution $G(D)$ on the basis of eq 9 and to the hydrodynamic radius distribution $f(R_h)$ by using the Stokes-Einstein equation, $R_h = k_B T / (6\pi\eta D)$, where k_B is the Boltzmann constant.

Experimental Section

Sample Preparation. The details of the PNIPAM preparation were described before.^{34,35} In the following, we only outline the basic procedure in the preparation of the PNIPAM samples: *N*-isopropylacrylamide (purchased from Eastman Kodak) monomer was recrystallized three times in a benzene/*n*-hexane mixture; the purified monomer (18 g) was dissolved in 150 mL of benzene with 1 mol % recrystallized azobisisobutyronitrile added as initiator; and this solution was degassed through three cycles of freezing and thawing. Polymerization was carried out at 56 °C for 30 h under a positive nitrogen pressure. The solvent was removed by evaporation and the polymer was further purified. The final yield was ~75%. The PNIPAM was fractionated twice by precipitation from an extremely carefully dried acetone solution to *n*-hexane at $T \sim 25$ °C. It should be emphasized that the use of the dried solvents is one of the key factors for the success in preparing a narrowly distributed PNIPAM sample. A careful combination of both the fractionation and filtration enabled us to prepare two very narrowly distributed ($M_w/M_n < 1.05$) high molecular weight PNIPAM samples. Hereafter, they are denoted as PNIPAM-1 ($M_w = 1.08 \times 10^7$ g/mol) and PNIPAM-2 ($M_w = 1.21 \times 10^7$ g/mol). With these PNIPAM samples, we prepared and clarified the extremely dilute PNIPAM aqueous solutions ($C \sim 5 \times 10^{-6}$ g/mL) with a 0.5- μ m filter. The resistivity of the distilled deionized water used as solvent in this study was 18.3 M Ω cm.

Laser Light Scattering. A commercial LLS spectrometer (ALV/SP-150) equipped with an ALV-5000 digital time correlator was used with a solid-state laser (ADLAS DPY425II, output power ~400 mW at $\lambda = 532$ nm) as the light source. The incident light beam was vertically polarized with respect to the scattering plane, and the intensity was regulated with a beam attenuator (Newport M-925B) so as to avoid localized heating in the light scattering cuvette. In our setup, the coherent factor β in dynamic LLS was ~0.87, a rather high value for an LLS spectrometer to be used for both static and dynamic LLS simultaneously. This is one of the reasons why we were able to carry out dynamic LLS in such an extremely dilute solution with a good signal-to-noise ratio. With some proper modifications,³¹ our LLS spectrometer is capable of measuring both static and dynamic LLS continuously in the range of 6–154°. The accessible small-angle range is particularly useful in the measurement of high molecular weight polymer chains because in static LLS the condition of $R_g q < 1$ is required to determine the precise value of R_g , whereas in dynamic LLS the extrapolation of $q \rightarrow 0$ and the interference of the internal motions associated with the long polymer chain in dynamic LLS can be avoided.³⁶ In addition, in this accessible small-angle range, the scattered intensity for the high molecular weight polymer is much stronger than at high scattering angles, so that we are able to study an extremely dilute solution. The typical long-term temperature stability inside our LLS sample holder was $\sim \pm 0.02$ °C.

Results and Discussion

Figure 1 shows the PNIPAM chain dimensions R as

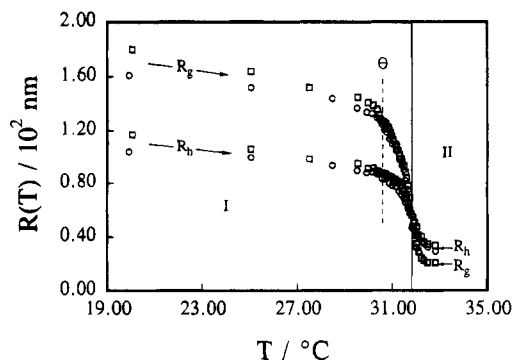


Figure 1. Change of the PNIPAM chain dimension as a function of the solution temperature, where \circ represents both the radius of gyration R_g and the hydrodynamic radius R_h for PNIPAM-1 and \square represents the same for PNIPAM-2. The dashed line indicates the Flory Θ temperature. The thermodynamically stable one-phase and kinetically stable two-phase region are respectively denoted as I and II.

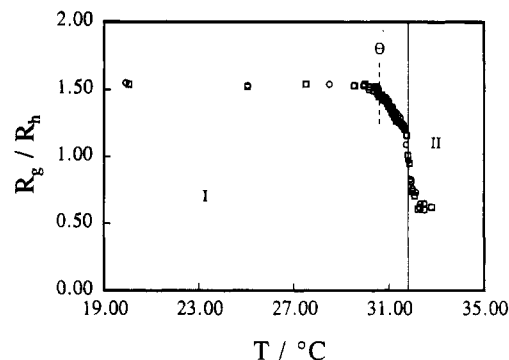


Figure 2. R_g/R_h as a function of the solution temperature, where all symbols have the same meanings as in Figure 1.

a function of the solution temperature, where “ \circ ” represent both the radius of gyration R_g and the hydrodynamic radius R_h for PNIPAM-1 and “ \square ”, for PNIPAM-2. Regions I and II refer to the thermodynamically stable one-phase region and kinetically stable two-phase region, respectively; i.e., in region II, individual PNIPAM chains first collapsed to densely packed single-chain globules which were only stable for a limited time period ($\sim 10^2$ min) and then these globules were thermodynamically driven to aggregate so that the system entered a two-phase region. Figure 1 shows that in the region of $T < \Theta$ the chain slightly shrinks as T increases and both R_g and R_h are linear functions of T . When $T > \Theta$, the PNIPAM chain starts to collapse and both R_g and R_h decrease dramatically as $(T - \Theta)$ increases. Figure 1 also shows that when the temperature changes from 20 to 33 °C, the PNIPAM chain dimension changes in terms of R_g decreases ~ 8 times whereas the decrease of R_h is much less in this temperature range, i.e., only ~ 3.5 times. This difference between the changes of R_g and R_h is understandable because they are defined in quite different ways. R_g is related to the actual space reached by the polymer chain, while R_h is only the radius of an equivalent hard sphere which has an identical diffusion coefficient D as the polymer chain in the solution. When the polymer chain is in an extended coil form, the water molecules in its occupied space are draining when the polymer chain diffuses, so that R_h is much smaller than R_g . In the collapsed state, the water molecules inside the globule are less draining so that R_h becomes smaller than R_g .

Figure 2 shows R_g/R_h as a function of the temperature, where all symbols and labels have the same

meanings as in Figure 1. Figure 2 shows that the plots of R_g/R_h vs T for two different molecular weights have collapsed into a single line, which is expected because R_g/R_h depends only on the chain conformation, not on the molecular weight, as predicted and experimentally verified.^{19,32,33} Figure 2 shows that, when $T < \Theta$, R_g/R_h is a constant (~ 1.52) even though both R_g and R_h decrease with increasing T as shown in Figure 1. The value of ~ 1.52 is close to the predicted value for a flexible coil in a good solvent,³² which means that when $T < \Theta$ the PNIPAM chain in water behaves like a random coil in a good solvent and the conformation is T -independent. Figure 2 shows also that, when $T > \Theta$, R_g/R_h first decreases linearly with increasing T and then drops just before entering the two-phase region II. A combination of Figures 1 and 2 shows that the linear decrease of R_g/R_h in this region is mainly due to the fast decrease in R_g . We attribute this linear decrease of R_g/R_h to the chain crumpling process, whereby a polymer coil contracts toward its center and the chain segments at the center and near the surface of the coil should contract simultaneously. Both of the contractions lead to the decrease in R_g , while R_h is mainly affected by the contraction near the surface. As the coil contracts, the chain density increases and most of the water molecules inside the collapsed coil will be nondraining. Therefore, the collapsed coil with the water molecules caged inside will become more and more like a hard sphere. R_h should gradually approach to the actual outside dimension of the collapsed coil, and the decrease in R_h will slow down. At present, it is not clear why R_g/R_h decreases linearly with T in that region. At $T \approx 32^\circ\text{C}$ where $R_g \approx R_h$, the PNIPAM solutions entered the two-phase region II. In this region, R_g and R_h were measured in the kinetically stable state, before the collapsed globules had a chance to aggregate. In the kinetically stable region II, R_g/R_h dropped from ~ 1 to a plateau value of ~ 0.62 . It is worth noting that R_g/R_h has dropped below 0.774, the predicted value for a uniform sphere. In the past, this point was repeatedly taken as a criterion of whether a given polymer coil had reached a globule state with a uniform density.^{9,20,21} But this prediction of $R_g/R_h = 0.774$ assumed a uniform density for the collapsed globule. The plateau value (~ 0.62) indicates that this assumption is incorrect, suggesting that during the collapse of the PNIPAM in water segments in the center of the coil contract faster than those near the surface. This leads to a higher density in the center of the globule. This observation is thermodynamically reasonable because the chemical potential of water has to continuously decrease from the outside of the coil to its center as its microscopic concentration is decreased. It should be noted that this lower plateau value can also be seen in Figure 4 of ref 20. However, it was overlooked there.

Figure 3 shows the scattered light intensity $I(\theta=15^\circ)$ as a function of temperature, where all symbols and labels have the same meanings as in Figure 1. According to eq 6, $I(q)$ at a fixed scattering angle should be nearly T -independent as long as there is no change in M_w and C , where we have assumed that n and dn/dc do not change too much in the small range of T . This T -independence of $I(q)$ is shown in Figure 3 when $T < \Theta$. However, when $T > \Theta$, but still in the stable region I, $I(q)$ started to decrease. First, we were astonished by this unexpected and strange intensity decrease since if there is aggregation $I(q)$ should increase. This cannot be explained by the possible change of dn/dc , R_g , or A_2

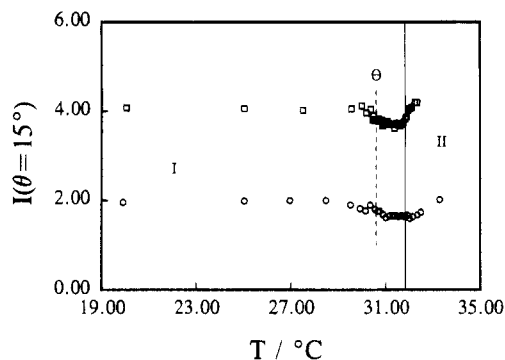


Figure 3. Scattered light intensity $I(\theta=15^\circ)$ as a function of the temperature, where all symbols and labels have the same meanings as in Figure 1.

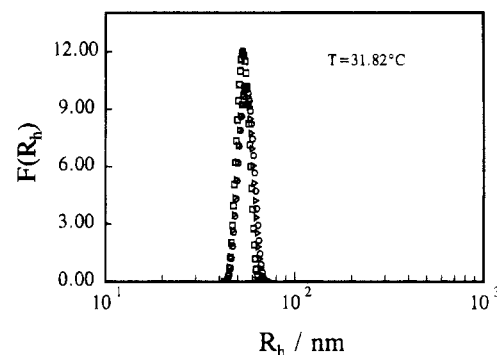


Figure 4. Hydrodynamic radius distribution $f(R_h)$ of PNIPAM-1 at different standing times after the PNIPAM solution was brought from 30.59 (the Θ temperature) to 31.82 $^\circ\text{C}$ (still in the thermodynamically stable region I). \circ $t = 5$ h; \triangle , 33 h; and \square , 44 h.

according to eq 6 because in the PNIPAM chain collapse, R_g decreases, A_2 becomes more negative, and dn/dc (if there are any changes) might increase slightly. Eventually, we speculated that the decrease of $I(q)$ may be attributed to the multiple scattering inside the collapsed PNIPAM globule in which the microscopic C is higher even though the macroscopic C is very low. The light scattered from the segments located at the center of the coil might be blocked by the segments near the surface when the scattered light travels from the coil center to the surface. Nevertheless, Figure 3 shows that in region I PNIPAM is thermodynamically stable in water and there is no aggregation between the PNIPAM molecules. On the other hand, in region II, $I(q)$ increases with T , which indicates aggregation of collapsed single-chain globules. According to eq 6, LLS is an extremely sensitive method to detect aggregates in a given polymer solution because $I(q)$ is directly proportional to the square of the mass M of the scatterer. Thus, Figure 3 supports our previous claim that the PNIPAM solution is thermodynamically stable in region I, while the solution is only kinetically stable in region II. This can be further demonstrated by our dynamic LLS results.

Figure 4 shows the hydrodynamic radius distribution $f(R_h)$ of PNIPAM-1 at different times (t) after the solution was brought from 30.59 (the Θ temperature) to 31.82 $^\circ\text{C}$ (still in the thermodynamically stable region I). In terms of the distribution width and peak position, the t -independence of $f(R_h)$ indicates that the PNIPAM in water at $T = 31.82^\circ\text{C}$ is thermodynamically stable. Moreover, $f(R_h)$ shows that the PNIPAM used in this study is narrowly distributed. In contrast, when $T > 32.01^\circ\text{C}$, we saw a very slow aggregation process.

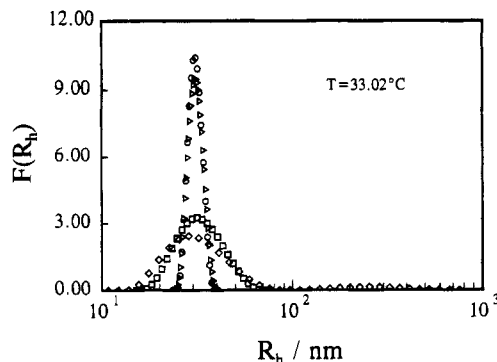


Figure 5. Typical slow aggregation process [in terms of $f(R_h)$] after the same PNIPAM solution used in Figure 4 was brought from 30.59 to 33.02 °C, where \circ , $t = 280$ s; Δ , 1850 s; \square , 3690 s; and \diamond , 3.44 h.

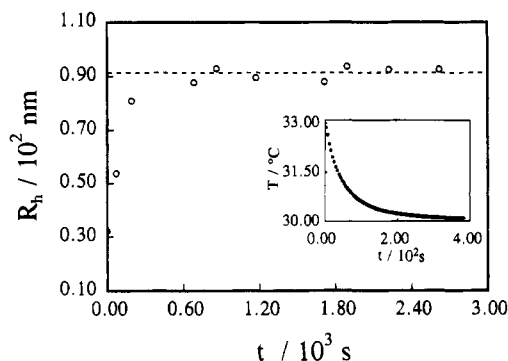


Figure 6. Dissolving kinetics (in terms of R_h) of the highly collapsed single-chain (PNIPAM-1) globule, where t is the standing time after the solution temperature was quenched from 33.02 to 30.02 °C and the dashed line represents the thermodynamically stable size of the PNIPAM-1 coil at 30.02 °C.

Figure 5 shows a typical slow aggregation process [in terms of $f(R_h)$] after the same PNIPAM solution used in Figure 4 was brought from 30.59 to 33.02 °C. No aggregation can be detected in the PNIPAM solution up to $t = 1850$ s. After standing at 33.02 °C for ~ 1 h, $f(R_h)$ gradually broadened. When $t = \sim 3.44$ h, a second peak with a larger size appeared in $f(R_h)$. The height of the second peak was low and represented the aggregates presumably made of individual collapsed single-chain globules. We found that the aggregation rate slowed as the solution temperature approached ~ 32.00 °C. After a set of careful experiments, we concluded that the phase transition temperature for the PNIPAM solution was $\sim 32.00 \pm 0.05$ °C. Next, we will present the kinetic studies of the collapsing and dissolving processes of single PNIPAM chains in water.

Figure 6 shows the dissolving kinetics (in terms of R_h) of the highly collapsed single-chain (PNIPAM-1) globule, where t is the standing time after the solution temperature was quenched from 33.02 to 30.02 °C. The experimental procedure was that first the stable PNIPAM solution was prepared at 30.02 °C and its R_h was determined (the dashed line in Figure 6); then the solution temperature was increased to 33.02 °C and stayed at 33.02 °C for $\sim 10^3$ s, so that individual PNIPAM chains only had time to collapse into the highly compacted single-chain globule, with no aggregation among the globules (as shown in Figure 5); and finally, the solution temperature was quenched from 33.02 to 30.02 °C, and both R_h and t were immediately recorded after the temperature change. The inset in Figure 6 shows how fast the solution temperature was

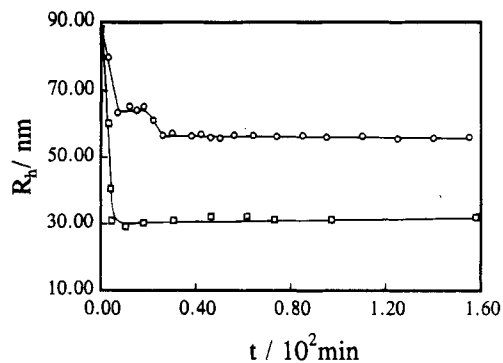


Figure 7. Collapsing kinetics after the PNIPAM-1 solution was jumped from 30.59 °C, respectively, to 31.82 (○) and 33.02 °C (□). The lines were drawn simply to guide the eye.

able to reach the equilibrium value, wherein a very special LLS cuvette made of a thin-wall (~ 0.4 mm) glass tube was used for all kinetic studies. Figure 6 shows that the process of the globule \rightarrow the extended coil (the dissolving kinetics) is too fast to be detected in our LLS setup; i.e., before the solution reached its temperature equilibrium at 30.02 °C the highly collapsed PNIPAM globule already expanded into an extended coil. This fast dissolving time ($< \sim 300$ s) indicates that there is no extensive chain knotting even inside the highly collapsed globule.

Figure 7 shows the PNIPAM chain collapsing kinetics after the PNIPAM-1 solution was jumped from 30.59 °C, respectively, to 31.82 and 33.02 °C, where the temperature jump took ~ 400 s. In the case of jumping from 30.59 to 33.02 °C (already inside the thermodynamically metastable, but kinetically stable two-phase region II), the collapse was too fast to be followed. Before the solution reached its temperature equilibrium, the chain had already collapsed. This fast collapsing process might further indicate that no extensive knotting exists in the collapsed globule because the knotting should be a slow process, especially inside the highly collapsed globule. When the temperature jumped to 31.82 °C (still in the thermodynamically stable region I), the chain collapsed (the decrease of R_h) followed a very interesting two-stage process. The first stage is too fast to be accurately recorded, so that it would be difficult for us to quantitatively analyze the data in Figure 7. The estimated time scales for these two stages are ~ 50 and ~ 300 s, respectively. To our knowledge, this is the first time that two-stage collapsing kinetics was ever observed in the thermodynamically stable region. We might attribute the first stage as a simple contraction of the PNIPAM chain, which can be considered as a proportional shrinking of the extended coil so that most of the existing topological constraints at 30.59 °C were "frozen" inside the contracted coil since the process is very fast. However, this contracted coil conformation is not thermodynamically stable at 31.82 °C, so that the PNIPAM chain has to relax into a thermodynamically stable conformation at 31.82 °C, possibly by the crumpling predicted by Grosberg and Kuznetsov.¹² In comparison with the collapsed globule at 33.02 °C, the thermodynamically stable globule at 31.82 °C is twice as large. If taking the R_h at 31.82 °C and the R_h at 33.02 °C respectively as R_{crum} and R_{eq} in eq 5, we are able to obtain $\zeta \sim 4.6$, which is smaller than the reported data (7–11) for polystyrene in cyclohexane.^{9,12,14}

Figure 8 shows a plot of the static expansion factor α_s as a function of the relative temperature Θ/T , where

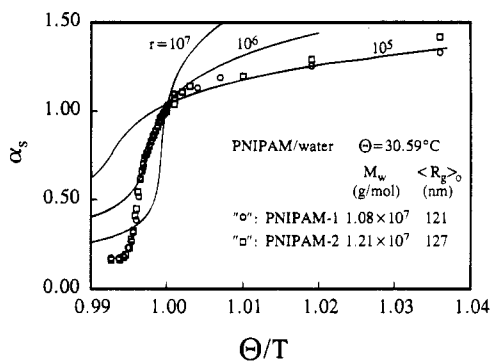


Figure 8. Plot of the static expansion factor α_s as a function of the relative temperature Θ/T , where α_s is defined as $R_g(T)/R_g(\Theta)$. \circ (PNIPAM-1) and \square (PNIPAM-2) are the measured results; and the lines, the calculated data from eq 1 with three different r values. If $M_0 = 113$ (the mass of the repeat unit), we have $r \sim 10^5$ for PNIPAM-1 and PNIPAM-2.

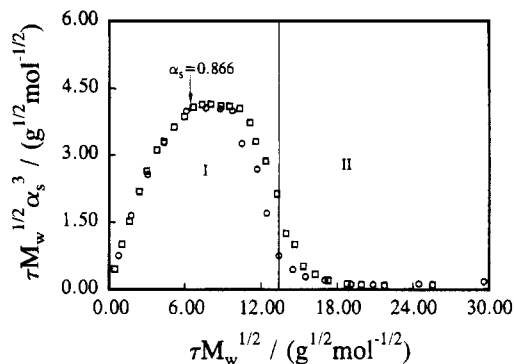


Figure 9. Plots of the scaled static expansion factor $\alpha_s^3 \tau M_w^{1/2}$ as a function of the reduced temperature $\tau M_w^{1/2}$ at $T > \Theta$ for PNIPAM-1 (\circ) and PNIPAM-2 (\square) in water.

α_s is defined as $R_g(T)/R_g(\Theta)$. When $T < \Theta$, the experimental results are reasonably represented by the line with $r = 10^5$. A similar result has been observed for polystyrene in cyclohexane.^{19,34} The theory works well in a good solvent wherein ϕ_0 is expected to be a weak function of T . On the other hand, when $T > \Theta$, the measured α_s drops much faster than the line with $r = 10^5$. We do not understand this discrepancy. Apparently, the results can be partially fitted by the line with $r = 10^6$. The remarkable point is that α_s decreases to a much lower plateau than predicted in eq 1. This might be because the hydrophobic and hydrophilic interactions in water are much stronger than those predicted by theory.

Figures 9 and 10, respectively, show the plots of the scaled expansion factor $\alpha_s^3 \tau M_w^{1/2}$ and $\alpha_h^3 \tau M_w^{1/2}$ as a function of $\tau M_w^{1/2}$. Such plots have been reported before for polystyrene in different organic solvents and also for PNIPAM in water.^{7,15} Several points in Figures 9 and 10 should be noted. We observed a well-established plateau for each PNIPAM sample. The plateau values in Figure 10 are very close to the estimate of ~ 0.6 from eq 2, but the plateau values in Figure 9 are $\sim 50\%$ lower than the estimate. The ratio of the plateau value in Figure 10 to that in Figure 9 is ~ 1.45 , which is much lower than $(1.481/1.161)^3 \sim 2$ predicted before²⁰ but close to the experimental values (~ 1.44) for polystyrene in various of organic solvents.⁷ Also, $\alpha_s^3 \tau M_w^{1/2}$ drops at higher $\tau M_w^{1/2}$ (still in the thermodynamically stable one-phase region I), which contradicts the prediction of eq 2. This paradox leads us to reexamine the conditions on which eqs 1 and 2 were derived. In eqs 1 and 2, the possible changes in the attractive interactions were not

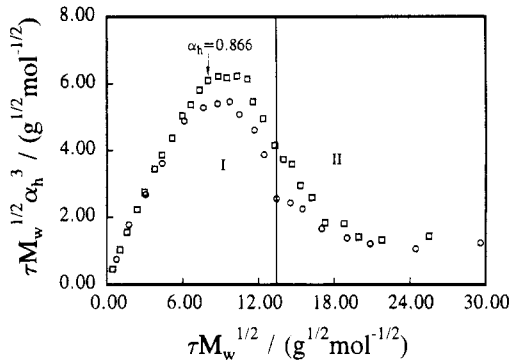


Figure 10. Plots of the scaled hydrodynamic expansion factor $\alpha_h^3 \tau M_w^{1/2}$ as a function of the reduced temperature $\tau M_w^{1/2}$ at $T > \Theta$ for PNIPAM-1 (\circ) and PNIPAM-2 (\square) in water, where $\alpha_h \equiv R_h(T)/R_g(\Theta)$.

included. However, in the highly collapsed globule this assumption might be violated, wherein the attractive interaction between different segments should be much stronger than in the extended coil conformation. This might explain why there is a drop followed by a plateau and might also be the reason for the fast decay in Figure 8 after $T > \Theta$. According to eq 2, when $d(\alpha^3 \tau M_w^{1/2})/d\alpha \sim 6\alpha^5 - 8\alpha^7 = 0$, i.e., $\alpha = 0.866$, the scaled expansion factor $\alpha^3 \tau M_w^{1/2}$ should reach a maximum, as observed in Figures 9 and 10. This agreement shows that eq 2 works quite well until the plateau is reached.

Finally, we would like to discuss the chain density in the globule. Our results show that even in the mostly collapsed globule where $R_g/R_h \sim 0.62$ the estimated chain density ρ is only ~ 0.2 g/cm³, where we used the simple approximation of $\rho \sim M_w/[N_A(4/3)\pi R_h^3]$. This means that the PNIPAM globule still contains $\sim 80\%$ of water.

Conclusion

With the success of preparing two narrowly distributed high molecular weight poly(*N*-isopropylacrylamide)s, we have accomplished the studies of the coil-to-globule transition of the individual PNIPAM chain in extremely dilute solution. We have, for the first time, demonstrated that a thermodynamically stable single-chain globule state can be experimentally reached. Our results showed that R_g/R_h decreases linearly as the solution temperature increases when T is higher than the Flory Θ temperature and that R_g/R_h can be lower than 0.774 predicted for a uniform sphere, which might indicate that even in the highly collapsed globule the chain density might not be uniform. The observed relaxation times (~ 10 – 10^2 s) for the disentanglement of a highly collapsed PNIPAM globule and the collapse of an extended PNIPAM coil were too short to support the previously proposed knotting process in the coil-to-globule transition. In addition, the highest chain density reached in the collapsed globule is only 0.2 g/cm³, which is significantly lower than that in bulk (~ 1 g/cm³). This implies that the collapsed globule contains $\sim 80\%$ water. All of our results indicate that there should be no high-degree knotting inside the collapsed globule. Finally, our results in terms of both the expansion (or say, contraction) factor α and the scaled expansion factor $\tau M_w^{1/2} \alpha^3$ indicate that the modified Flory theory for the polymer chain expansion (contraction) works well in a good solvent and near the Θ temperature, but failed in the region where the chain is highly collapsed. The theory has to be further modified to include the strong attractive interaction inside the collapsed single-chain globule.

Acknowledgment. Special thanks to Prof. Morawetz, H. for his valuable comments and proof reading of the manuscript. The financial support of the RGC (the Research Grants Council of Hong Kong Government) Earmarked Grant 1994/95 (CUHK 299/94P, 221600260) and the Special Summer Research Grant 1995 from CUHK are gratefully acknowledged.

References and Notes

- (1) Stockmayer, W. H. *Makromol. Chem.* **1960**, *35*, 54.
- (2) Ptitsyn, O. B.; Kron, A. K.; Eizner, Y. Y. *J. Polym. Sci., Part C* **1968**, *16*, 3509.
- (3) Yamakawa, H. *Modern Theory of Polymer Solutions*; Harper & Row: New York, 1971.
- (4) Grosberg, A. Y.; Kuznetsov, D. V. *Macromolecules* **1992**, *25*, 1996, and references therein.
- (5) Yamakawa, H. *Macromolecules* **1993**, *26*, 5061.
- (6) Post, C. B.; Zimm, B. H. *Biopolymers* **1979**, *18*, 1487; **1982**, *21*, 2123.
- (7) Park, I. H.; Wang, Q. W.; Chu, B. *Macromolecules* **1987**, *20*, 1965.
- (8) Chu, B.; Park, I. H.; Wang, Q. W.; Wu, C. *Macromolecules* **1987**, *20*, 2883.
- (9) Chu, B.; Yu, J.; Wang, Z. L. *Prog. Colloid Polym. Sci.* **1993**, *91*, 142.
- (10) Tanaka, F. *J. Chem. Phys.* **1985**, *85*, 4707.
- (11) Tanaka, F.; Ushiki, H. *Macromolecules* **1988**, *21*, 1041.
- (12) Grosberg, A. Y.; Kuznetsov, D. V. *Macromolecules* **1993**, *26*, 4249, and the references therein.
- (13) Yu, J.; Wang, Z. L.; Chu, B. *Macromolecules* **1992**, *25*, 1618.
- (14) Chu, B.; Ying, Q. C.; Grosberg, A. Y. *Macromolecules* **1995**, *28*, 180.
- (15) Chan, H. S.; Dill, K. A. *Phys. Today* **1993**, *46*, 24.
- (16) Post, C. B.; Zimm, B. H. *Biopolymers* **1982**, *21*, 2139.
- (17) Lerman, L. S. *Proc. Natl. Acad. Sci. U.S.A.* **1971**, *68*, 1886.
- (18) Lerman, L. S.; Allen, S. L. *Cold Spring Harbor Symp. Quant. Biol.* **1973**, *38*, 59.
- (19) Yamamoto, I.; Iwasaki, K.; Hirotsu, S. *J. Phys. Soc. Jpn.* **1989**, *58*, 210.
- (20) Kubota, K.; Fujishige, S.; Ando, I. *J. Phys. Chem.* **1990**, *94*, 5154.
- (21) Meewes, M.; Ricka, J.; de Silva, M.; Nyffenegger, R.; Binkert, Th. *Macromolecules* **1991**, *24*, 5811.
- (22) Schild, H. G. *Prog. Polym. Sci.* **1992**, *17*, 163, and references therein.
- (23) de Gennes, P.-G. *J. Phys. Lett.* **1975**, *36*, L55.
- (24) Sanchez, I. C. *Macromolecules* **1979**, *12*, 276.
- (25) Akcasu, A. Z.; Han, C. C. *Macromolecules* **1979**, *12*, 980.
- (26) Chan, H. S.; Dill, K. A. *J. Chem. Phys.* **1994**, *100*, 9238.
- (27) de Gennes, P. G. *J. Phys. Lett.* **1985**, *46*, L-639.
- (28) Grosberg, A. Yu.; Nechaev, S. K.; Shakhovich, E. *J. Phys. Fr.* **1988**, *49*, 2095.
- (29) Zimm, B. H. *J. Chem. Phys.* **1948**, *16*, 1099.
- (30) Debye, P. *J. Phys. Colloid Chem.* **1947**, *51*, 18.
- (31) Pecora, R. *Dynamic Light Scattering*; Plenum Press: New York, 1976.
- (32) Chu, B. *Laser Light Scattering*, 2nd ed.; Academic Press: New York, 1991.
- (33) Stockmayer, W. H.; Schmidt, M. *Pure Appl. Chem.* **1982**, *54*, 407; *Macromolecules* **1984**, *17*, 509. =
- (34) Zhou, S. Q.; Fan, S. Y.; Au-yeung, S. T. F.; Wu, C. *Polymer* **1995**, *36*, 1341.
- (35) Wu, C.; Zhou, S. Q. *Macromolecules* **1995**, *28*, 5388.
- (36) Wu, C.; Chan, K.; Xia, K. Q. *Macromolecules* **1995**, *28*, 1032.
- (37) Huber, K.; Bantle, S.; Lutz, P.; Burchard, W. *Macromolecules* **1985**, *18*, 1461.
- (38) Nordmeier, E.; Lechner, D. *Polym. J.* **1989**, *21*, 623.
- (39) Slagowski, E. L. Ph.D. Thesis, University of Akron, Akron, OH, 1972.

MA950461I